Available online at www.sciencedirect.com
SCIENCE DIRECT®
Journal of Non-Crystalline Solids 333 (2004) 291–295
JOURNAL OF NON-CRYSTALLINE SOLIDS
www.elsevier.com/locate/jnoncrysol

Nanoindentation investigation of amorphous hydrogenated carbon thin films deposited by ECR-MPCVD

Sheng-Rui Jian [a], Te-Hua Fang [b,*], Der-San Chuu [a]

[a] Institute and Department of Electrophysics, National Chiao Tung University, Hsinchu 300, Taiwan
[b] Department of Mechanical Engineering, Southern Taiwan University of Technology, Tainan 710, Taiwan

Received 29 October 2002; received in revised form 3 September 2003

Abstract

Nanomechanical properties of amorphous hydrogenated carbon thin films are performed by nanoindentation technique. The amorphous hydrogenated carbon films are produced on silicon substrate by electron cyclotron resonance microwave plasma chemical vapor deposition (ECR-MPCVD). The effect of negative bias voltage on amorphous hydrogenated carbon films is examined by Raman spectroscopy and the results showed that the intensity ratio of D-peak to G-peak (I_D/I_G) of amorphous hydrogenated carbon films at various bias voltages, increased as the bias voltage increased. The results also showed that Young's modulus and hardness also increased as the bias voltage increased. In addition, Young's modulus and hardness both decreased as the indentation depth increased.

1. Introduction

Amorphous hydrogenated carbon (a-C:H) films, also known as diamond-like carbon (DLC) films, have desirable performance due to their physical and chemical properties, such as optical transparency, high electronic resistivity, chemical inertness, high hardness and low surface energy [1–4]. Amorphous hydrogenated carbon thin films are a candidate for a wide range of applications as protective coatings in areas such as magnetic storage disks, biomedical coatings and microelectromechanical system (MEMS) [5–8].

Many deposition methods have been developed, including ion-beam sputtering, direct current and radio frequency (RF) magnetron sputtering, cathode arc deposition and plasma enhanced chemical vapor deposition [9–13]. Each method has its relative advantages for certain applications. Among them, electron cyclotron resonance microwave plasma chemical vapor deposition (ECR-MPCVD) is an excellent technique because of the superior plasma species production rate and low substrate temperature during deposition [14–17].

Nanoindentation testing is the most frequently used technique for measuring thin film properties such as Young's modulus and hardness within a sub-micron scale [18–20]. Therefore, this technique is expected to be useful for measurement of mechanical properties of thin films. Research in this area is partially summarized in references [21–24].

The aim of this study is to investigate the nanomechanical properties of amorphous hydrogenated carbon thin films deposited by the ECR-MPCVD at various substrate biases. Additionally, discussion of indentation mechanisms on a nanometer-scale and the influence of bias voltage on the deposited films are presented.

2. Experimental details and methodology

Amorphous hydrogenated carbon thin films are produced on silicon substrates by ECR-MPCVD, with RF bias being applied to the substrate holder. The films are prepared in an ECR-MPCVD system, with a mixture of methane and hydrogen reactant gases. A 13.56 MHz RF with a negative bias voltage is coupled to the substrate holder. The chamber is first evacuated to

* Corresponding author. Tel.: +886-6 253 3131x3543; fax: +886-6 242 5092.
E-mail address: fang@mail.stut.edu.tw (T.-H. Fang).

0022-3093/$ - see front matter © 2003 Elsevier B.V. All rights reserved.
doi:10.1016/j.jnoncrysol.2003.10.012

Table 1
Growth conditions of amorphous hydrogenated carbon thin films

Substrate	Silicon
Gas	H_2, CH_4
Pressure (Pa)	10^{-3}
Flow rate (sccm)	H_2: 30, CH_4: 30
Deposition time (min)	180
Microwave power (W)	70
RF bias (V)	−30, −50, −70

10^{-3} Pa, and then the methane/H_2 mixture is introduced for film deposition. The amorphous hydrogenated carbon thin films growth conditions are listed in Table 1. Further details of the deposition process can be found in Refs. [5,25].

The surface morphology of amorphous hydrogenated carbon thin films was examined using atomic force microscopy (AFM) under ambient conditions. AFM scanning uses only the two vertical quadrants to measure vertical deflection of the cantilever, and thus the surface profile of the specimen, i.e. topography. The R_a surface roughness was measured using the same device in contact mode. Nanomechanical properties such as Young's modulus and hardness of amorphous hydrogenated carbon thin films were obtained by nanoindentation. Load controlled indentation testing followed a trapezoidal loading profile with a hold time of typically 10 s at peak loads. Peak loads ranged from 100 to 1000 μN at loading rate of 10 μN/s. The diamond indenter was a Berkovich tip with a tip radius of 100 nm [19].

Amorphous hydrogenated carbon thin films were subjected to a depth-sensing nanoindentation, which is a reliable method [26,27] for measuring the mechanical properties of thin films. The typical continuous load–displacement curves are obtained from a Berkovich indenter. The area and the depth relationship of the Berkovich indenter is

$$A_c = 24.56h^2, \tag{1}$$

where A_c is the contact area and h is the calculated plastic depth. The constants assume a perfectly manufactured tip with a face angle of 65.3°. The contact area A_c was calculated from stiffness values obtained from the nanoindentation data.

In depth-sensing nanoindentation, the relationship between the stiffness and contact area is derived by

$$S = \beta \frac{2\sqrt{A_c}}{\pi} E^*, \tag{2}$$

where S is the measured stiffness and β is a shape constant of 1.034 for the Berkovich tip. The composite modulus, E^* is obtained by [19]

$$\frac{1}{E^*} = \frac{1-\nu_i^2}{E_i} + \frac{1-\nu_m^2}{E_m}. \tag{3}$$

Here ν and E represent Poisson's ratio and Young's modulus, respectively. The subscripts i and m refer to the indenter and test material. The indenter properties used in this study's calculations were $E_i = 1140$ GPa and $\nu_i = 0.07$ and assumed that Poisson's ratio was $\nu_m = 0.3$ for the amorphous hydrogenated carbon thin films.

The hardness of a material is defined as its resistance to local plastic deformation. Thus, the hardness, H, is determined from maximum indentation load P_{max} divided by the projected contact area [19]:

$$H = \frac{P_{max}}{A_c}. \tag{4}$$

To better understand the mechanism of plastic deformation on amorphous hydrogenated carbon thin films, the radius a, of the contact area to determine the stress is calculated by using the Hertzian equation [28]:

$$a = \left(\frac{3PR}{4E^*}\right)^{1/3}. \tag{5}$$

The contact stress–strain analysis revealed that the local strain on the thin film can be very useful to improving the quality of the films and also recognized the deformation mechanisms at a nanoscale under the micro-Newton level loads.

3. Results

The first-order Raman spectrum of single-crystalline graphite shows a sharp intense peak at 1581 cm^{-1}. This peak is assigned to the E_{2g} C–C stretching mode and is referred to as the G-peak [29]. In contrast, for polycrystalline graphite the peak is centered at 1350 cm^{-1} and is referred to as the D-peak [29]. It has been suggested that an additional type of diamond-like carbon exists, with a frequency of 1540 ± 20 cm^{-1} depending on the distortion from the graphite structure and the vibrational mode is mainly represented by C–C stretching [30]. Raman spectral analysis of the films grown with different substrate negative bias voltages reveals a diamond-like structure with a peak centered at approximately 1540 ± 20 cm^{-1} and a shoulder peak at approximately 1350 cm^{-1}, as shown in Fig. 1. On the whole, the films displayed the same typical Raman spectra of the DLC thin films presented in other reports [5,31].

From the fitting parameters, the peak position, peak width and integrated intensity ratio I_D/I_G is obtained. The intensity ratio of the D- and G-peaks, I_D/I_G, has been shown to correlate inversely with both the size and the density of the graphite crystallites. In Fig. 2, the I_D/I_G ratio increased as the negative bias was increased and the results showed that this phenomena lead to the formation of carbon films with less diamond-like structures. Therefore, increasing the negative bias volt-

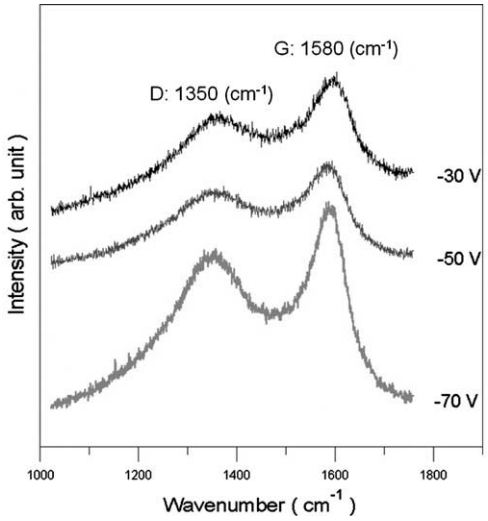

Fig. 1. Raman spectra of amorphous hydrogenated carbon thin films deposited with various substrate biases.

age will make the G-peak shift towards a higher frequency and decrease the sp^3-bonded in the DLC thin films.

Fig. 3(a)–(c) show that the surface topography for the amorphous hydrogenated carbon thin films, grown at the different bias voltages of −30, −50 and −70 V. The corresponding surface roughness R_a for −30, −50 and −70 V are 0.23, 0.28 and 0.29 nm, respectively. In addition, Fig. 4 shows the load–displacement curve and indent mark. The load–displacement curve on the amorphous hydrogenated carbon thin film was −50 V and a triangle indent can be observed in the indent mark having shallow depths. In addition to that, the amorphous hydrogenated carbon thin films have cracked due to their plastic behavior, which caused the atoms to 'pile-up' on either side of the indentation. This 'pile-up' phenomenon is found to be anisotropic and the

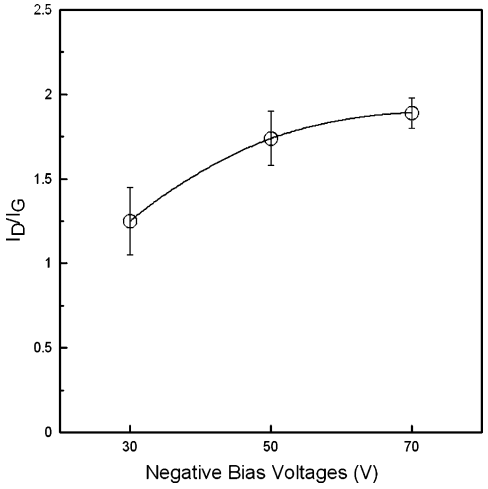

Fig. 2. The relationship of bias voltages and I_D/I_G ratio.

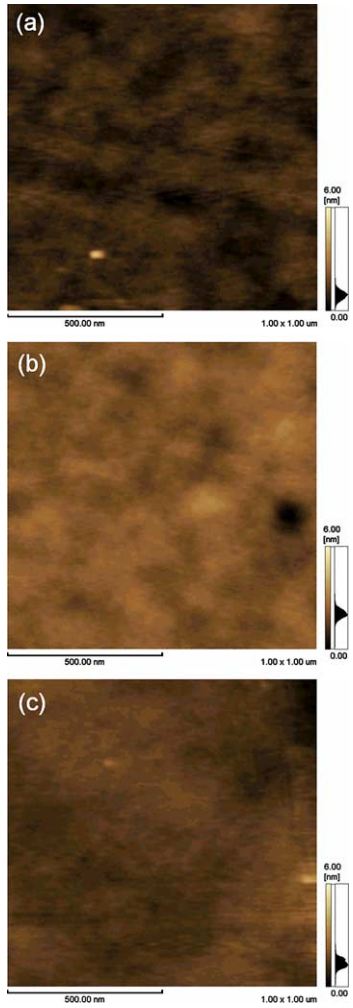

Fig. 3. (a)–(c) AFM images of amorphous hydrogenated carbon thin films at different bias voltages of −30, −50 and −70 V, respectively.

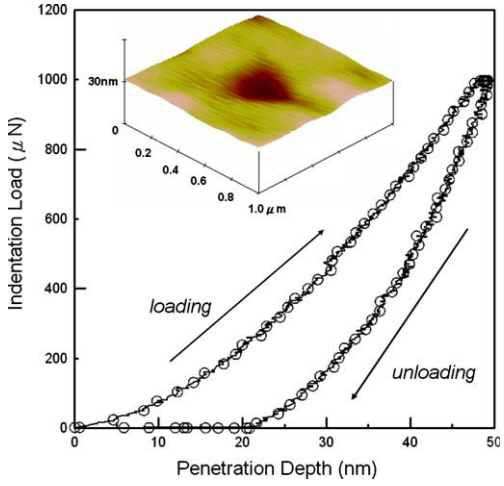

Fig. 4. A load–displacement curve and the indent AFM image of amorphous hydrogenated carbon thin film at −50 V bias voltage.

magnitude of the pile-up increases as the indentation load was increased. This phenomenon gives evidence of the plastic behavior on amorphous hydrogenated carbon thin films.

The Young's modulus of the amorphous hydrogenated carbon thin films can be derived during nanoindentation process by Eqs. (2) and (3) as above-mentioned. Young's modulus was obtained from the nanoindentation process at different applied loads and is shown in Fig. 5. The experiment results showed that the Young's modulus was 166.47 ± 1.53 to 173.82 ± 1.95, 168.61 ± 1.39 to 180.56 ± 3.44 and 175.34 ± 1.16 to 187.45 ± 2.55 GPa for the bias voltages of -30, -50 and -70 V, respectively. A plot of the estimated hardness as a function of plastic penetration depth for the three different bias voltages substrates is shown in Fig. 6. It is apparent that the hardness decreases as the applied load was increased. In addition, the corresponding hardness was 17.68 ± 0.22 to 18.96 ± 0.54, 18.82 ± 0.29 to 20.12 ± 0.58 and 19.52 ± 0.23 to 21.56 ± 0.64 GPa for -30, -50 and -70 V, respectively. This indicated that the Young's modulus and hardness increased as the bias voltage was increased and the highest value being obtained at a bias of -70 V.

The contact stress and contact strain relationships were deduced from the above-calculated data at the bias voltages shown in Fig. 7. The larger the stress, the larger the strain and therefore the deformation of the thin films subsequently lead to a yielding behavior. It can be seen that when the substrate bias voltage was increased it causes a larger contact stress and contact strain on the deposited films. In other words, the higher the negative bias voltage the more stress the deposited films could bear.

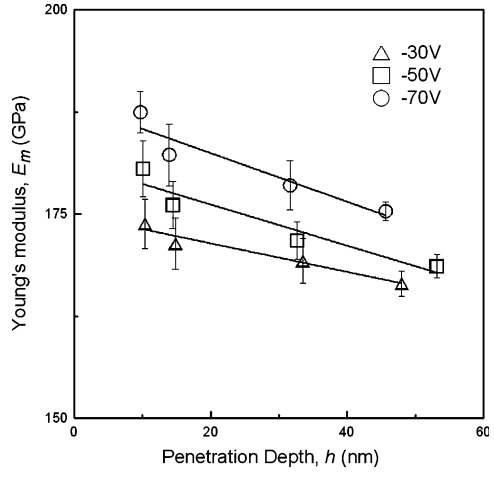

Fig. 5. Young's modulus of amorphous hydrogenated carbon films measured as a function of the penetration depth.

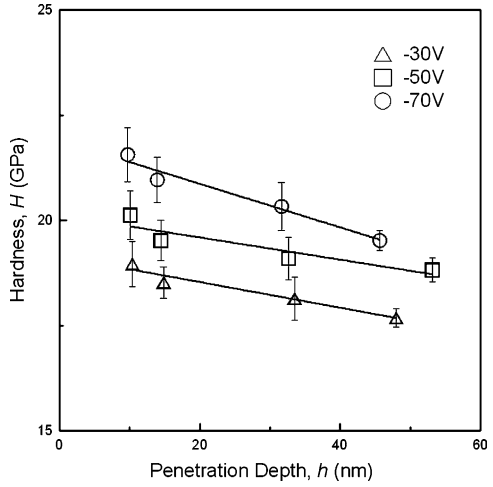

Fig. 6. Hardness of amorphous hydrogenated carbon films measured as a function of the penetration depth.

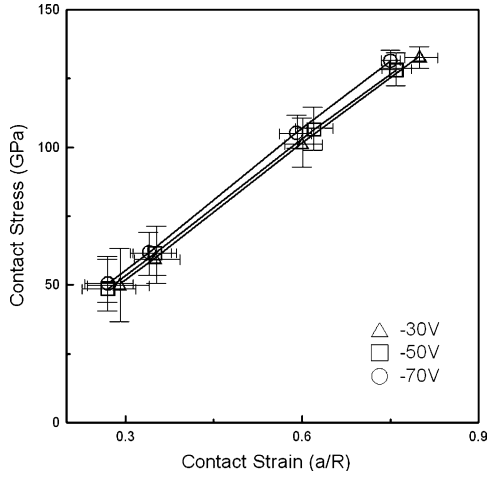

Fig. 7. Contact stress–strain relationship of amorphous hydrogenated carbon films with bias voltages.

4. Discussion

The Raman spectra measurement showed that the sp^3-bonding carbon clusters increased as the negative bias voltage was increased, which is consistent with the results in Ref. [32]. The properties of the amorphous hydrogenated carbon thin films deposited by ECR-MPCVD were improved by the effects of negative bias voltages.

The structure of the amorphous hydrogenated carbon thin films has a strong dependence on the ion energy, because the ion energy is proportional to the bias voltage of the cathode and the ions in the capacitive coupled RF plasma were accelerated by the negative bias voltage. The results indicated that the different bias voltages caused the bias energies bombarding the surface of the growing films, to have had a major influence on the amorphous hydrogenated carbon films. The increased quantity of

sp^3-bonded carbon and the increased number of areas of high strain caused by the increased bias voltages and thereby increased ion energy had a beneficial effect on the amorphous hydrogenated carbon thin films. Also when looking at the amorphous hydrogenated carbon thin films microstructures, the number of small islands decreased as the increasing bias voltage was increased. So, as the bias voltage was increased, more sp^3-bonded carbon was created. The sp^3-bonded carbon exhibits the properties of diamond, such as a lower friction coefficient and higher harnesses [33]. Nanoscale mechanism was mainly caused by the interaction of the surface atoms and the sub-surface atoms, including the stretching or breaking of interatomic bonds. Hence the nanoscale characteristics and mechanisms were clearly shown with the aid of nanoindentation measurements.

5. Conclusion

In summary, it was demonstrated that the nanomechanical properties of amorphous hydrogenated carbon thin films that were deposited by ECR-MPCVD at different substrate biases had improved microstructure and nanomechanical properties. The Raman spectra showed that all the deposited films, regardless of the substrate bias, exhibit two characteristical peaks centered at 1350 and 1580 cm^{-1}. In addition, it was found that increasing the negative bias voltage caused the G-peak to shift towards a high frequency and the D-peak to shifts towards a lower frequency causing the ratio of I_D/I_G to be increased. The nanoindentation experiment results showed that the presence and level of bias voltage on the substrate plays a significant role in the nanomechanical properties of amorphous hydrogenated carbon thin films deposited on silicon wafers.

Acknowledgements

This work was partially supported by the National Science Council, Taiwan, under grant nos. NSC90-2218-E218-011 and NSC91-2212-E-218-007.

References

[1] Z.H. Liu, J.F. Zhao, J. McLaughlin, Diamond Relat. Mater. 8 (1999) 56.
[2] A. Grill, V. Patel, Diamond Relat. Mater. 2 (1993) 597.
[3] A. Grill, B.S. Meyerson, in: K.E. Spear, J.P. Dismukes (Eds.), Synthetic Diamond: Emerging CVD Science and Technology, Wiley, New York, 1994, p. 91 (Chapter 5).
[4] R. Memming, H.J. Tolle, P.E. Wierenga, Thin Solid Films 143 (1986) 31.
[5] X.T. Zhou, S.T. Lee, I. Bello, A.C. Cheung, D.S. Chiu, Y.W. Lam, C.S. Lee, K.M. Leung, X.M. He, Surf. Coat. Technol. 123 (2000) 273.
[6] Z. Jiang, C.J. Lu, D.B. Bogy, C.S. Bhatia, T. Miyamoto, Thin Solid Films 258 (1995) 75.
[7] J. Robertson, Thin Solid Films 383 (2000) 81.
[8] P. Goglia, J. Berkowitz, J. Hoehn, A. Xidis, L. Stover, Diamond Relat. Mater. 10 (2001) 271.
[9] S. Neuville, A. Matthews, MRS Bull. 22 (1997) 22.
[10] J.J. Cuomo, J.P. Doyle, J. Bruley, J.C. Liu, Appl. Phys. Lett. 58 (1991) 1.
[11] R. Wei, P.J. Wilbur, A. Erdemir, F.M. Kustas, Surf. Coat. Technol. 51 (1992) 139.
[12] C. Weissmantel, K. Bewilogua, K. Breuer, D. Dietrich, U. Ebersbach, H.-J. Erier, B. Rau, G. Reisse, Thin Solid Films 96 (1982) 31.
[13] K. Miyoshi, J.J. Pouch, S.A. Alterovitz, Mater. Sci. Forum 52&53 (1989) 645.
[14] A.A. Voevodin, M.S. Donley, J.S. Zabinski, Surf. Coat. Technol. 92 (1997) 42.
[15] H. Ronkainen, J. Koskinen, A. Anttila, K. Holmberg, J.-P. Hirvinen, Diamond Relat. Mater. 1 (1992) 639.
[16] H. Dimgen, C.P. Klages, Surf. Coat. Technol. 49 (1991) 543.
[17] M. Zarrabian, N. Fourches-Coulon, G. Turban, M. Lancin, C. Marhic, Diamond Relat. Mater. 6 (1997) 542.
[18] J.B. Pethica, R. Hutchings, W.C. Oliver, Philos. Mag. A 48 (1983) 593.
[19] N.R. Moody, W.W. Gerberich, N. Burnham, S.P. Baker, Fundamentals of Nanoindentation and Nanotribology, Materials Research Society, 1998.
[20] C.M. Yang, Mater. Chem. Phys. 41 (1995) 295.
[21] G.E. Fougere, L. Riester, M. Ferber, J.R. Weertman, R.W. Siegel, Mater. Sci. Eng. A 204 (1995) 1.
[22] Z. Hung, L.Y. Gu, J.R. Weertman, Scripta Mater. 37 (1997) 1071.
[23] W.C. Oliver, G.M. Pharr, J. Mater. Res. 7 (1992) 1564.
[24] M.F. Doerner, D.S. Gardner, W.D. Nix, J. Mater. Res. 7 (1986) 845.
[25] T.H. Fang, C.I. Weng, M.J. Chiang, Diamond Relat. Mater. 11 (2002) 1653.
[26] S.R. Jian, T.H. Fang, D.S. Chuu, J. Electron. Mater. 32 (2003) 496.
[27] L. Valentini, E. Braca, J.M. Kenny, L. Lozzi, S. Santucci, J. Non-Cryst. Solids 291 (2001) 153.
[28] K.L. Johnson, Contact Mechanics, Cambridge University, Cambridge, 1985.
[29] F. Tuinstra, J.L. Koenig, J. Chem. Phys. 53 (1970) 1126.
[30] P.V. Houng, Diamond Relat. Mater. 1 (1991) 33.
[31] H. Tsai, D.B. Bogy, J. Vac. Sci. Technol. A 5 (1987) 3287.
[32] J.F. Chang, H.Y. Ueng, T.F. Young, Y.C. Wang, W.C. Hwang, Surf. Coat. Technol. 157 (2002) 179.
[33] X. Li, B. Bhushan, Wear 220 (1998) 51.